Vapor phase tri-methyl-indium seeding system suitable for high temperature spectroscopy and thermometry.

Whiddon, Ronald; Zhou, Bo; Borggren, Jesper; Aldén, Marcus; Li, Zhongshan

Published in:
Review of Scientific Instruments

DOI:
10.1063/1.4930123

2015

AIP | Review of Scientific Instruments

Vapor phase tri-methyl-indium seeding system suitable for high temperature spectroscopy and thermometry

R. Whiddon, B. Zhou, J. Borggren, M. Aldén, and Z. S. Li

Citation: Review of Scientific Instruments **86**, 093107 (2015); doi: 10.1063/1.4930123
View online: http://dx.doi.org/10.1063/1.4930123
View Table of Contents: http://scitation.aip.org/content/aip/journal/rsi/86/9?ver=pdfcov
Published by the AIP Publishing

Vapor phase tri-methyl-indium seeding system suitable for high temperature spectroscopy and thermometry

R. Whiddon, B. Zhou, J. Borggren, M. Aldén, and Z. S. Li[a)]
Division of Combustion Physics, Lund University, P.O. Box 118, S-221 00 Lund, Sweden

(Received 6 April 2015; accepted 23 August 2015; published online 14 September 2015)

Tri-methyl-indium (TMI) is used as an indium transport molecule to introduce indium atoms to reactive hot gas flows/combustion environments for spectroscopic diagnostics. A seeding system was constructed to allow the addition of an inert TMI laden carrier gas into an air/fuel mixture burning consequently on a burner. The amount of the seeded TMI in the carrier gas can be readily varied by controlling the vapor pressure through the temperature of the container. The seeding process was calibrated using the fluorescent emission intensity from the indium $6^2S_{1/2} \rightarrow 5^2P_{1/2}$ and $6^2S_{1/2} \rightarrow 5^2P_{3/2}$ transitions as a function of the calculated TMI seeding concentration over a range of 2–45 ppm. The response was found to be linear over the range 3–22.5 ppm; at concentrations above 25 ppm there is a loss of linearity attributable to self-absorption or loss of saturation of TMI vapor pressure in the carrier gas flow. When TMI was introduced into a post-combustion environment via an inert carrier gas, molecular transition from InH and InOH radicals were observed in the flame emission spectrum. Combined laser-induced fluorescence and absorption spectroscopy were applied to detect indium atoms in the TMI seeded flame and the measured atomic indium concentration was found to be at the ppm level. This method of seeding organometallic vapor like TMI to a reactive gas flow demonstrates the feasibility for quantitative spectroscopic investigations that may be applicable in various fields, e.g., chemical vapor deposition applications or temperature measurement in flames with two-line atomic fluorescence. © *2015 AIP Publishing LLC.* [http://dx.doi.org/10.1063/1.4930123]

I. INTRODUCTION

Atomic indium is an oft considered tracer, together with atomic thallium, lead, and gallium, for the determination of temperatures in flame when using the two-line atomic fluorescence technique,[1–3] as it features spin-orbit components of the atomic ground state that have a significant population at flame temperatures. The most common approach for introducing indium atoms into gas phase uses an indium chloride/water solution, which is either directly aspirated (pneumatic/acoustic) or injected through a capillary into the combustion zone. In this seeding process, small droplets of indium chloride solution are produced, which then evaporate, forming $InCl_3$ crystals. These crystals decompose when passing through the flame front, producing atomic indium. Inherently, indium signal can only be obtained from the post combustion region of the flame.[4] The use of liquid seeding systems in flame measurements introduces various complications to the combustion system. Aspirating seeders generate a range of droplet sizes, only some of which successfully join the carrier gas stream; excess must be drained off to diminish problems of clogging and condensation on instrument surfaces. In pneumatic nebulizers, small fluctuations in the driving pressure can result in noticeable changes in the seeding concentration over time. The combustion environment may be influenced by the use of solvent based seeding systems, due to changes in flame temperature or flame chemistry.[5–7] Recently, Manteghi *et al.*[8] reported seeding of $InCl_3$ powder with a smart particle seeding design, the conversion to indium atoms is still limited to hot region but the utilization of solvent solution was circumvented. Investigations have also been made to seed indium atoms in a flow stream by laser ablation of metallic indium, with detection of the ground state indium via laser-induced fluorescence.[9,10] While it surmounts the clogging and solvent problems of liquid seeding systems, there are limitations due to the added complexity of a high energy laser system and the propensity of the ablation process to generate a limited amount of indium atoms together with various sized particles.

We have investigated the suitability of the organometallic compound tri-methyl-indium (TMI) as a seed source for indium in a combusting flow. TMI is an organically linked metal that is used in vapor deposition of semiconductor devices and nanoparticle synthesis in flame. It is a high vapor pressure, pyrophoric, crystalline compound which melts at 88 °C and becomes unstable above 140 °C.[11] In this work, an indium seeding system was constructed using a commercial TMI sublimation chamber originally designed for application in chemical vapor deposition. The feasibility of TMI as a vapor phase transport for introducing indium into a combustion environment was demonstrated by detecting the fluorescent emission from indium atoms and indium containing radicals produced during the combustion process. The concentration of the indium atoms in the post-flame region was measured by tunable diode laser absorption spectroscopy (TDLAS) and laser-induced fluorescence (LIF).

[a)]Email address: Zhongshan.Li@forbrf.lth.se

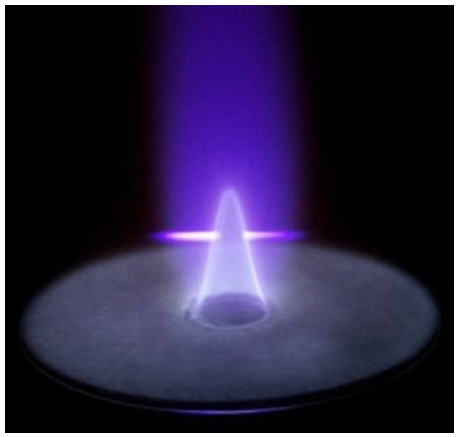

FIG. 1. Photo of a premixed methane/air flame ($\phi = 1.0$) seeded with 10 ppm TMI. A narrow 410 nm laser beam sent horizontally from left to right through the flame is manifested by laser-induced fluorescence from indium atoms.

II. SETUP

A. Combustion system

The experiments discussed in Secs. II A and II B were performed on a McKenna burner with a central open jet, as shown in Figure 1. The burner features a water cooled, 6 cm diameter, sintered brass frit which surrounds a 1 cm diameter open central tube. The respective fuel/air mixtures are regulated by means of mass flow controllers. The brass frit section of the burner is supplied with methane and air which are mixed at an equivalence ratio of $\phi = 0.9$ prior to combustion. Mass flow controllers were also used to regulate the supply of nitrogen, oxygen, and methane to the central jet. The three gases were mixed several meters upstream of the burner surface. Nitrogen was also used as the carrier gas for the seeding apparatus; this flow was introduced to the central jet flow 15 cm upstream of the burner surface. Changes in the carrier gas flow rate were compensated for by adjustment of the nitrogen component of the central jet flow. The beam from a diode laser (line width narrowed with an external cavity) tuned to 410 nm was sent through the flame. The path of the laser beam is clearly shown via LIF from indium atoms, as illustrated by the photo in Figure 1.

B. Seeding system

Schematics of the TMI seeding system and the burner are shown in Figure 2. At the heart of the system is a stainless steel TMI sublimation chamber sourced from Sigma-Aldrich, which was submersed in a chilled water/antifreeze bath. The chamber function is described by Gerrard[12] and was used in the standard flow configuration for this application. Stainless steel 6 mm tubing, valves, and junctions from Swagelok were used to construct the seeding system. Metal seat, sealed bellows type valves were used to eliminate possible leakage of air into the system through the valve stems. Nitrogen was used as the carrier gas to transport the TMI vapor to the burner. The flow of nitrogen was controlled using a mass flow controller upstream of the TMI chamber. The arrangement of valves and junctions allows for the TMI chamber to be selectively bypassed without interruption of the carrier gas flow. A Bosch turbo-molecular pump is connected to a four way junction upstream of the TMI chamber. By bypassing the TMI chamber it was possible to remove contaminants, e.g., water, oxygen, or residual TMI, by repeatedly flushing the system with nitrogen for a period several minutes followed by evacuating the system. This process was repeated three times before first use of the seeding system and after any exposure of the seeding system to air. A back flow prevention valve was placed between the seeding system and the central jet flow to prevent the air/fuel mixture from contaminating the system in the event of a pressure imbalance between the two flows. The TMI carrier gas is introduced to the burner fuel/air flow 15 cm before the burner surface.

The concentration of TMI at the burner was adjusted by changing the flow through the TMI bubbler, as this afforded a wider range of seeding concentrations than temperature variation. The vapor pressure of TMI in the carrier flow is calculated using Equation (1),[13]

$$\log_{10}(P) = 10.11 - \left(\frac{3204}{T}\right) \tag{1}$$

with the vapor pressure of TMI (P) in kPa, temperature (T) in Kelvin. The concentration of TMI (C_{TMI}) in the jet flame can then be calculated by the dilution of the TMI containing carrier gas and the fuel, nitrogen and oxygen flows of the central burner jet according to Equation (2),

$$C_{TMI} = \left(\frac{P_{TMI}V_{carrier}}{760}\right)/(V_{carrier} + V_{N_2} + V_{O_2} + V_{CH_4}), \tag{2}$$

where V indicates the volume flow of the specified component.

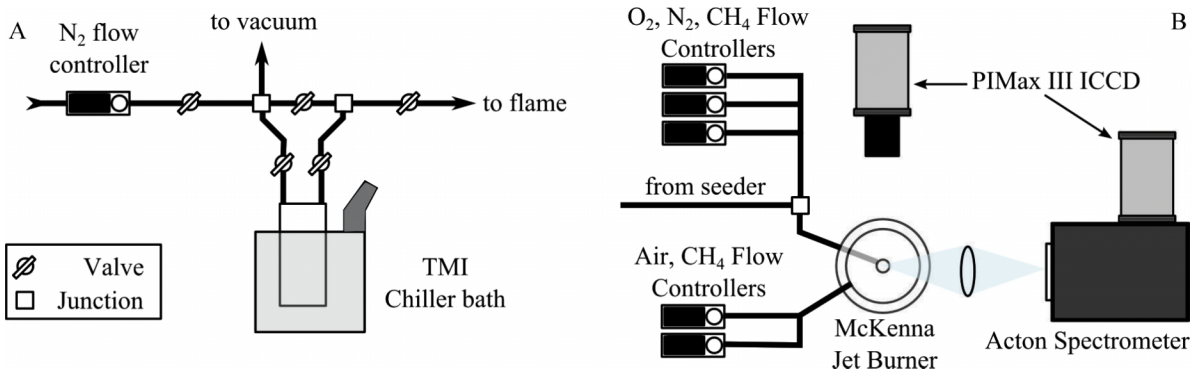

FIG. 2. TMI seeding apparatus (a) and burner assembly (b). The PI Max III ICCD camera was used both in spectrometric methods as detector and for two dimensional imaging.

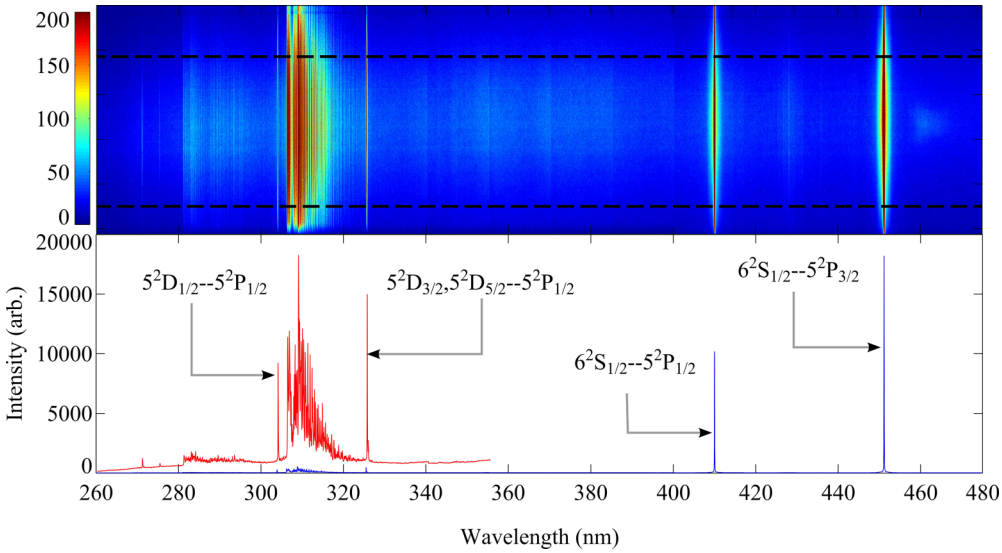

FIG. 3. Flame spectrum from a horizontal slice of the flame located 26 mm above the burner surface for 10 ppm TMI seeding. Above: 2-D spectrum showing the spatial distribution of the spectral features, radial position in the vertical axis, and wavelength on the horizontal axis. Note the intensity range is relative and the 410 nm and 451 nm indium transitions are saturated. Below: average spectrum from the region between the two dashed lines in the upper image with selected indium transitions labelled. A factor of 20 magnification of the spectral intensity in the 260-340 nm spectral range is shown in red.

III. APPLICATIONS

A. Atomic indium emission for flame TMI seeding calibration

Flame spectral emissions were collected by a 500 mm f/2.0 Halle lens installed at two focal distances from the flame center and formed a one-to-one image of the flame onto the plane containing the entrance slit of an Acton 1/2-m spectrometer. The aforementioned PI Max III camera was used as detector; the spectral sensitivity was corrected using a tungsten calibration lamp. The emission spectrum from a stoichiometric central jet flame seeded with 10 ppm TMI is shown in Figure 3. The measurement region was located at the radial center of the jet flame, 26 mm above the burner surface; the area was defined by the dimensions of the spectrometer inlet (100 μm × 1 cm). This point was slightly above the tip of the flame cone. A 1200 mm^{-1} grating was used to record a series of high resolution sub-spectra. The ICCD integration time was 10 s for each high resolution spectrum. The two dimensional spectrum is averaged over the region marked by the two broken lines to create the plot shown in the lower half of Figure 3. Several characteristic spectral lines have been identified using the NIST spectral database for indium.[14] Featuring most prominently in the spectrum are the two atomic indium lines generated by the $6^2S_{1/2} \rightarrow 5^2P_{1/2}$ and $6^2S_{1/2} \rightarrow 5^2P_{3/2}$ transitions at 410 and 451 nm, respectively. Using a 20 times magnification of the 260-340 nm region of the spectrum, bands of the OH A-X transitions and additional indium transitions are visible: 304 nm ($5^2D_{1/2} \rightarrow 5^2P_{1/2}$) and a doublet at 325 nm ($5^2D_{3/2}$; $5^2D_{5/2} \rightarrow 5^2P_{1/2}$).

The relation of the TMI concentration in the fuel/air stream to the seeding flow rate, as indicated by the intensity of the indium emission, is shown in Figure 4. The emission intensities from the $6^2S_{1/2} \rightarrow 5^2P_{1/2}$ and $6^2S_{1/2} \rightarrow 5^2P_{3/2}$ transitions as recorded in Figure 3 were evaluated for each measurement. Intensity values were corrected for the ICCD efficiency in the respective wavelength regions. The calculated seeding concentration of TMI supplied to the central jet flame at $\phi = 1.0$ was varied from 2.5 to 45 ppm. The concentration changes were achieved by adjusting the flow rates through the TMI chamber to reach the desired concentration as determined by Equation (2). The sequence of TMI concentrations tested was not serial, i.e., measurements were alternated at high and low concentration settings, in order to demonstrate any memory effects. The upper range of linear response for TMI seeding concentration is 25 ppm; at higher seeding concentrations the signal falls below linearity. There was a persistent indium emission signal, equivalent to a 1-2 ppm TMI seeding level, being observed, indicating the existence of TMI deposition in the pipe line.

As the two transitions arise from the same upper energy level, the intensity is predicted by the probability of each transition which for the transitions in question should be 0.56, and in absence of self-absorption this ratio should be

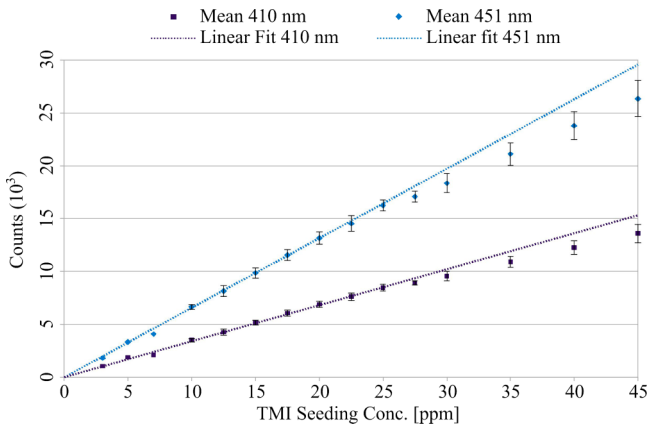

FIG. 4. Mean integrated emission intensity for the 410 nm and 451 nm indium transitions as a function of TMI seeding concentration. Lines represent the linear regression for response from 0-25 ppm of TMI seeding.

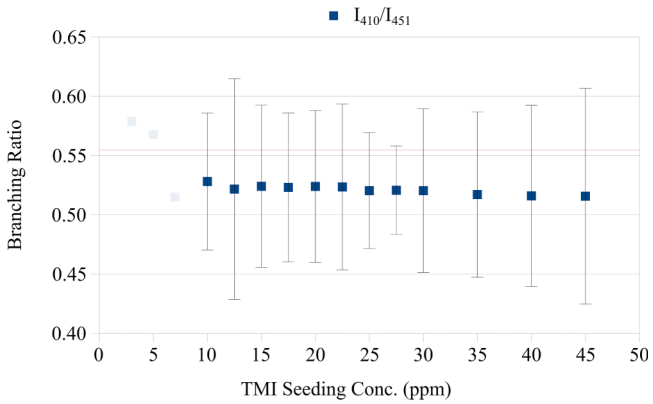

FIG. 5. Branching ratio from observed indium transition intensities as a function of TMI seeding concentration. Error is commuted from individual intensity measurements in Fig. 4.

constant.[15] Figure 5, which depicts the calculated branching ratio of the $6^2S_{1/2} \rightarrow 5^2P_{1/2}$, $5^2P_{3/2}$ of indium transitions, shows a slight decrease in the branching ratio at increasing concentrations of TMI. However, for all TMI seeding concentrations the branching ratios were observed within one standard deviation of the expected value, indicating the insignificance of self-absorption for the present experimental condition.

B. Absorption and laser-induced fluorescence from indium atoms

1. Imaging using laser-induced fluorescence

Atomic transitions generally have high absorption cross-sections and fluorescence quantum efficiencies compared to molecules and even low power diode lasers can induce a strong fluorescence signal useful for diagnostic purposes such as temperature measurements.[15–17] An external cavity diode laser (ECDL, Toptica DL100-Pro) tuned to the $6^2S_{1/2} \rightarrow 5^2P_{1/2}$ transition of indium was used to conduct laser-based measurements on TMI seeded flames, to obtain the distribution of indium atoms throughout the flame and the concentration. Shown in Figure 6 is a LIF image in the previously described TMI seeded conical flame taken with an intensified CCD camera. The external cavity diode laser has a line width of a few hundred kHz and a mode-hop free tuning range of approximately 25 GHz. The distribution of indium in the flames was investigated by capturing the LIF using the ICCD camera placed perpendicular to the laser beam path. An interference filter centered at 450 nm was used to detect the non-resonant fluorescence and to reduce background flame emission in the images. The condition of the investigated methane/air premixed flame was, as previously described, a stoichiometric TMI seeded conical flame surrounded by a lean co-flow flame with $\Phi = 0.9$. The LIF signal is seen in the upper part of Figure 6 for a flame seeded with 5 ppm of TMI from the inner jet.

The radial distribution of the LIF signal bounded by dashed red lines is shown in the lower portion of Figure 6. The laser beam was sent from left to right and the TMI was seeded only to the center jet. It is obvious that the In atoms

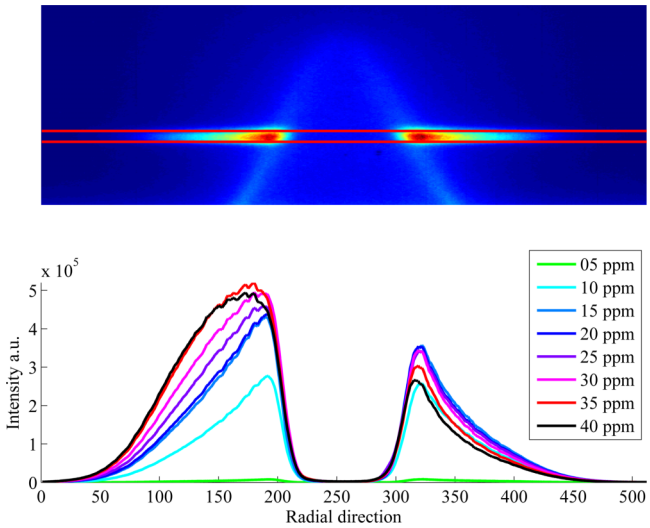

FIG. 6. Laser-induced fluorescence imaged across a methane air conical flame with 5 ppm TMI seeding. Lower chart is the integrated LIF signal over the fluorescing area for different TMI seeding concentrations.

were released after the seeded flow passes the pre-heat zone of the flame. If the concentration of seeded TMI is sufficiently low so the absorption of the laser beam is negligible, the fluorescence signal is proportional to the indium distribution in the flame and a symmetric LIF distribution will be observed, see, e.g., 5 ppm TMI seeding in Fig. 6. The shape of the indium concentration distribution, characterized by a peak near the reaction zone and decay to the pilot coflow lean flame, reflects the combined effects of molecular diffusion and In atom oxidization. As the TMI seeding concentration increased above 10 ppm, absorption of the excitation laser beam can be clearly observed. The strong LIF signal over the complete flame region clearly shows the feasibility of laser-based indium measurements for laser diagnostics.

2. Concentration measurements using absorption spectroscopy

According to Beer-Lambert's law the transmitted intensity, I, through an absorbing media is related as

$$I = I_0 e^{-\sigma l N}, \tag{3}$$

where I_0 is the incident power, σ is the absorption cross-section, l the absorption path length, and N the number density of the absorbing species. The absorption cross-section for the $6^2S_{1/2} \rightarrow 5^2P_{1/2}$ transition is calculated from the Einstein A coefficient,

$$\sigma(\nu) = \frac{A\lambda^2 g(\upsilon - \nu_0)}{8\pi} \frac{2J+1}{2J'+1}, \tag{4}$$

where λ is the wavelength of the transition, g is the normalized line shape function, and J is the J quantum number of each state. For low concentrations, it can be assumed that the detected fluorescence is proportional to the local absorption and the path length can estimated from the acquired image of the laser-induced fluorescence as seen in Figure 6. Threshold values above the background intensity yield the absorption path length and the averaged concentration can be obtained.

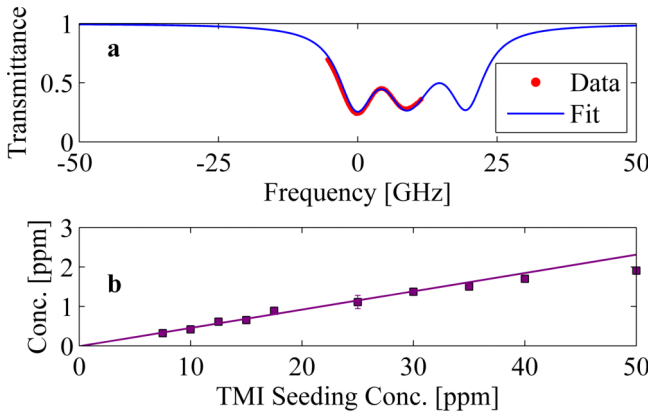

FIG. 7. (a) Red line: recorded transmittance profile for TMI seeding concentration 15 ppm, averaged over 50 wavelength scans; blue line: best fit. (b) Measured concentration as a function of the calculated concentration from Equation (2). The trend is similar to that of Figure 4 with a linear correlation between seeding concentration and measured concentration, the line is a linear fit to the data up to 25 ppm. The error bar is the estimated uncertainty coming from the line-averaged temperature, uncertainty in fit, and absorption path length.

A photo-diode placed after the flame measured the absorption of the laser beam, while the ECDL was tuned over the hyperfine structure of indium for several different concentrations of TMI seeding. A background signal was acquired with the TMI seeding system turned off. Part of the laser beam was directed to a confocal Fabry-Perot etalon with a free-spectral range of 1 GHz to acquire a frequency scale, while the laser was tuned. Due to the limited mode-hop free scanning range of the diode laser, the entire line shape was not covered in the absorption measurement. A least-square fitting algorithm generating a theoretical line shape to the well-known hyperfine structure of indium was developed to fit the measured absorbance line shapes. Variable parameters in the fit were background, absorbance, temperature, and pressure broadening. In Figure 7(a), the recorded line shape and the best fit is shown and a good agreement is observed even though the fitting is done to a line shape exhibiting a wide range of temperatures along the line.

The measured indium concentration plotted against the calculated concentration from Equation (2) is shown in Figure 7(b) and a similar trend as in Figure 4 is observed characterized by a deviation from linearity above 25 ppm. The non-linear behavior is likely due to loss in saturating of the TMI flow when the mass flow is increased. For higher flow speeds, the residence time of the gas in the bubbler will decrease and thereby result in insufficient time for a saturated TMI vapor being formed. An estimated error due to uncertainties in the line averaged temperature, fitting of the line shape, and the estimated absorption path length is shown in the error bar in Figure 7(b). In order to estimate the TMI to In atoms conversion in this slightly lean flame, the concentration just after the reaction zone is estimated to be 1.5 ppm for the 10 ppm TMI seeding case, which yield an estimated conversion efficiency of around 15%.

C. Spectroscopy of various indium radicals

1. System settings

Experiments were performed to investigate an orange emission that was observed when TMI was transported by a nitrogen flow to the post combustion region of a fuel-rich premixed flame. The central jet flow of the previously described McKenna burner was supplied with nitrogen and TMI vapor. At TMI seeding concentrations of 10 ppm, a faint orange luminescence was observed. An image of the orange luminescence is seen in Figure 8(a). The luminescence was found to increase in intensity as the TMI seeding concentration increased. The orange luminescence was highly susceptible to quenching by the addition of oxygen to the central jet flow; similarly, the luminescence was only present when the flame surrounding the central jet flow was operated at an equivalence ratio above $\phi = 1.4$. A horizontal slice of the orange luminescence region of the flame 15 mm above the burner surface was imaged to the input slit of an imaging spectrometer. A spatially resolved spectrum of the horizontal image region in the orange luminescence zone is shown in Figure 8(b) (spatial coordinate is rotated 90° to the vertical axis to allow the spectral coordinate on the horizontal axis).

2. Spectral features

Some features held in common with lean flames (cf. Figure 3) can be easily identified, like OH and atomic In lines. The spectral features around the inner cones are of special interest in this spatially resolved spectrum. The congested cluster of bands that appear near 360 nm are believed to be caused by transitions of the molecule InOH.[18] High resolution

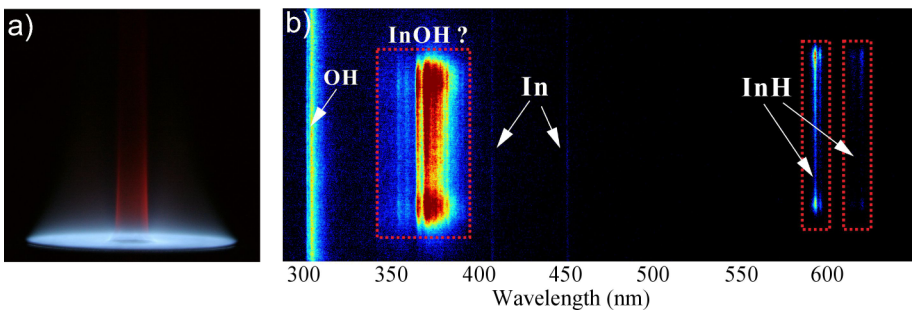

FIG. 8. (a) Photo of a flame with central jet feed with N_2 seeded with around 200 ppm TMI and the surrounding pilot flame operated at $\varphi = 1.4$. (b) Spectrum of the orange luminescence with spatial coordinate rotated 90° relative to the flame in (a).

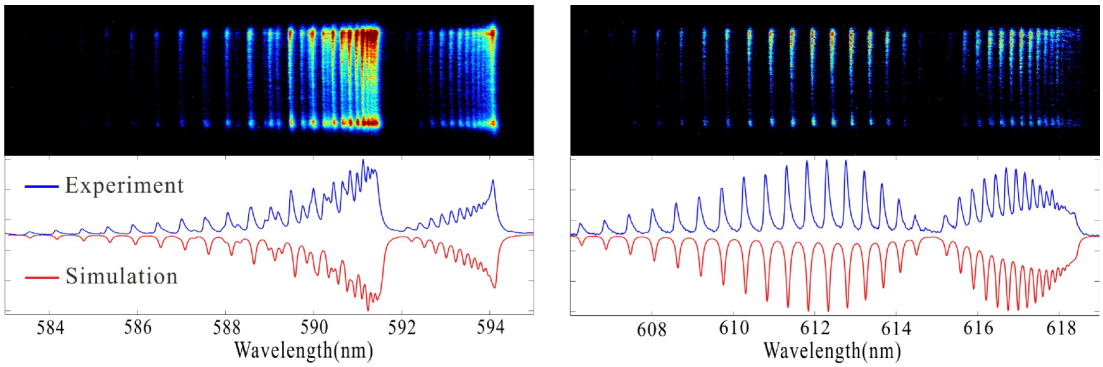

FIG. 9. High resolution spectra of InH transitions and corresponding predicted spectra from PGOPHER software.

spectra of the two band groups near 600 nm are shown in Figure 9. These emission bands have well resolved structure arising from InH transitions, this was confirmed by simulating the recorded spectra using the software PGOPHER.[19] For the simulation, a temperature of 580 K and a pure Lorentzian profile with 0.11 nm in line width were adopted to obtain the best fitting.

InH emission spectrum was observed from a King furnace as reported first by Grundström in 1938,[20] followed by extensive studies of the InH spectrum.[21–23] To the best of the authors' knowledge, the present work reports the first observation of InH emission spectrum in combustion environment. While further investigation of various indium compounds in the inert jet is ongoing, this is an exciting development as combustion synthesis is currently the most widely used means of nano-materials production.[24]

IV. CONCLUSION

This work was performed to assess the possibility of seeding indium into combustion environments without resorting to a liquid phase injection method. In that respect, there was marked success and the indium signal was present and uniformly distributed in the flame. Linearity in the indium emission signal as a function of the seeding concentration was observed up to 25 ppm of TMI seeding, which was also noticed in diode laser experiments. About 10% of the seeded TMI converted to atomic indium even at slightly lean flame conditions as measured by laser absorbance.

By carrying TMI into a reduction hot environment like a rich combustion environment, it was discovered that the TMI partially decomposed to InH and at least one other indium compound indicated by the presence of an orange luminescence. This presents the possibility of online spectroscopic monitoring of TMI concentrations in vapor deposition applications. This could also be of interest to the semiconductor community particularly in the area of flame fabrication of nano-materials.

The successful application of this indium seeding method drives further interest in two line atomic fluorescence temperature determination in the flame. This is a tried method that is still being actively developed both on the systems side and the application side. We are additionally looking at the feasibility of using other high vapor pressure compounds (e.g., tri-methyl-gallium) seeded in a similar manner to thermally map the lower temperature regions of the flame, especially the pre-heat zone of the flame.

ACKNOWLEDGMENTS

This work was supported by the Swedish Energy Agency, the Knut & Alice Wallenberg Foundation, the Swedish Research Council (VR), and the European Research Council.

[1]H. Haraguchi *et al.*, "Measurement of small volume flame temperatures by the two-line atomic fluorescence method," Appl. Spectrosc. **31**, 156–163 (1977).
[2]M. Aldén *et al.*, "Spatially resolved temperature measurements in a flame using laser-excited two-line atomic fluorescence and diode-array detection," Opt. Lett. **8**, 241–243 (1983).
[3]N. Omenetto *et al.*, "Color temperature atomic fluorescence method for flame temperature measurement," Anal. Chem. **44**(9), 1683–1686 (1972).
[4]J. Nygren *et al.*, "Applications and evaluation of two-line atomic LIF thermometry in sooting combustion environments," Meas. Sci. Technol. **12**, 1294–1303 (2001).
[5]J. H. Gibson, W. E. L. Grossman, and W. D. Cooke, "Excitation processes in flame spectrometry," Anal. Chem. **35**, 266–277 (1963).
[6]J. D. Winefordner and H. W. W. Latz, "Quantitative study of factors influencing sample flow rate in flame photometry," Anal. Chem. **33**, 1727–1732 (1961).
[7]Q. N. Chan *et al.*, "Solvent effects on two-line atomic fluorescence of indium," Appl. Opt. **49**, 1257–1266 (2010).
[8]A. Manteghi *et al.*, "Two-line atomic fluorescence thermometry in the saturation regime," Appl. Phys. B: Lasers Opt. **118**(2), 281–293 (2015).
[9]D. H. Gu. *et al.*, "Mechanism for laser-induced fluorescence signal generation in a nanoparticle-seeded flow for planar flame thermometry," Appl. Phys. B: Lasers Opt. **118**(2), 209–218 (2015).
[10]P. R. Medwell *et al.*, "Flow seeding with elemental metal species via an optical method," Appl. Phys. B: Lasers Opt. **107**(3), 665–668 (2012).
[11]Epichem, Trimethylindium, Material Safety Data Sheet, March 13, 2000.
[12]N. Gerrard, "An improved method of trimethylindium transport for the growth of indium phosphide and related alloys by MOVPE," J. Cryst. Growth **121**, 500–506 (1992).
[13]D. Shenaikhatkhate, R. Dicarlojr, and R. Ware, "Accurate vapor pressure equation for trimethylindium in OMVPE," J. Cryst. Growth **310**, 2395–2398 (2008).
[14]I. Johansson and U. Litzen, "The term systems of the neutral gallium and indium atorns derived from new measurements in the infrared region," Ark. Fysikum **34**, 573 (1967).
[15]J. Hult, I. S. Burns, and C. F. Kaminski, "Two-line atomic fluorescence flame thermometry using diode lasers," Proc. Combust. Inst. **30**, 1535–1543 (2005).
[16]J. Hult, I. S. Burns, and C. F. Kaminski, "Measurements of the indium hyperfine structure in an atmospheric-pressure flame by use of diode-laser-induced fluorescence," Opt. Lett. **29**(8), 827–829 (2004).

[17]I. S. Burns *et al.*, "A method for performing high accuracy temperature measurements in low-pressure sooting flames using two-line atomic fluorescence," Proc. Combust. Inst. **33**, 799–806 (2011).
[18]N. M. Lakin *et al.*, "The identification of InOH in the gas phase and determination of its geometric structure," J. Chem. Phys. **100**, 8546 (1994).
[19]C. M. Western, PGOPHER, a Program for Simulating Rotational Structure, University of Bristol, December 2, 2013.
[20]B. Grundström, "Band spectrum of indium hydride," Nature **141**, 555 (1938).
[21]M. L. Ginter, "The band spectrum of the InH molecule: Characterization of the a3Π state," J. Mol. Spectrosc. **11**, 301–320 (1963).
[22]K. F. Freed, "On the hyperfine structure of InH and the theory of the hyperfine structure of molecules in Hund's case (C)," J. Chem. Phys. **45**, 1714 (1966).
[23]L. Veseth, "The hyperfine structure of diatomic molecules: Hund's case (cα)," J. Mol. Spectrosc. **59**, 51–62 (1976).
[24]H. K. Kammler, L. Mädler, and S. E. Pratsinis, "Flame synthesis of nanoparticles," Chem. Eng. Technol. **24**, 583–596 (2001).